Supplementary information

Cancer-associated fibroblast compositions change with breast-cancer progression linking S100A4 and PDPN ratios with clinical outcome

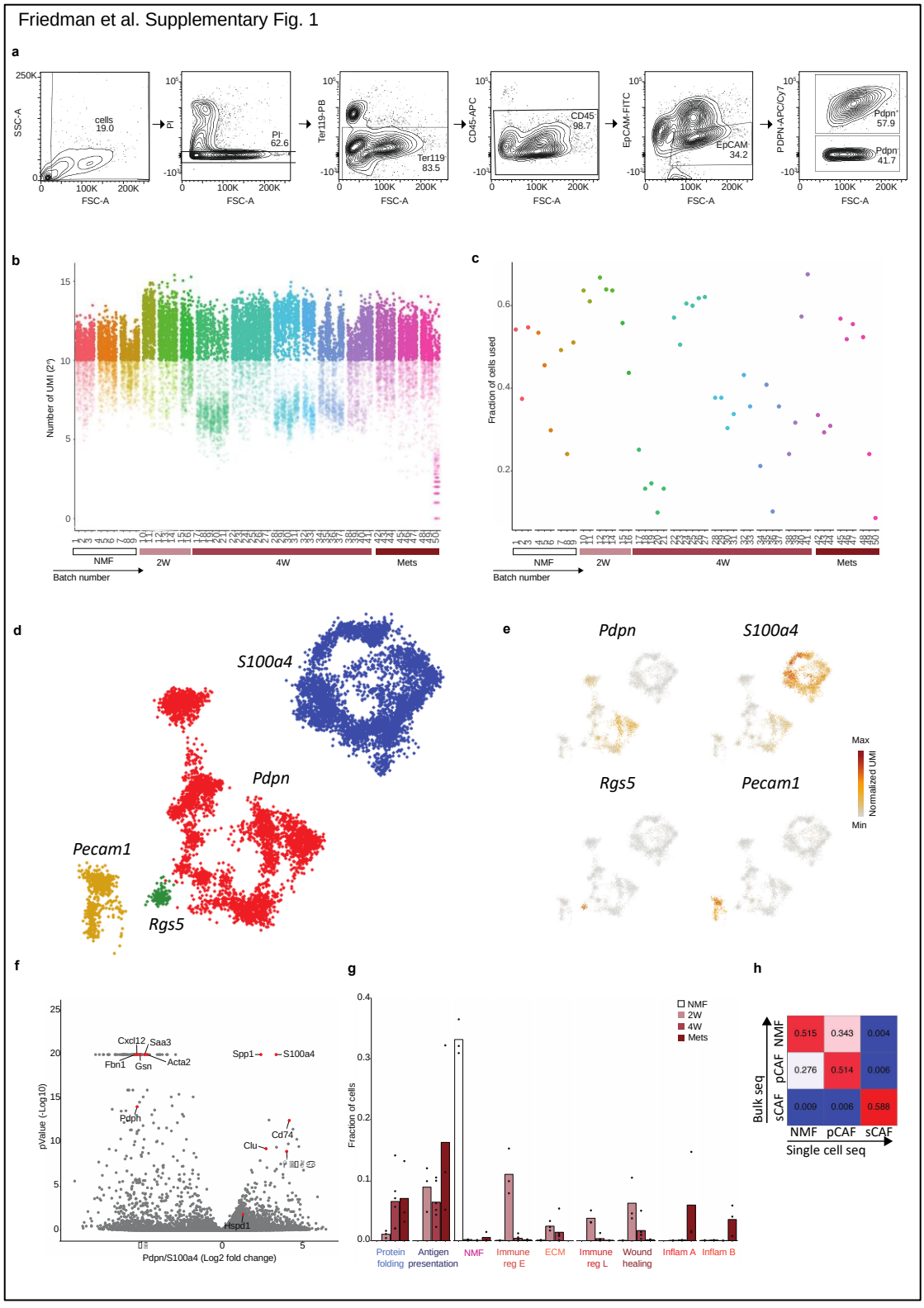

Supplementary Fig. 1: A single cell map of breast cancer stroma. a, Sorting strategy**:** All live single cells (PI negative cells after debris and doublet exclusion) staining negative for Ter119 (Red blood cells); CD45 (immune); and EpCAM (epithelial) were collected and single cell sorted. PDPN was used for index sorting of pCAFs. Representative flow cytometry plots are shown. **b-d,** Quality control metrics of single cells analyzed in this study. **b,** Total unique molecular identifier (UMI) per cell. Cells are grouped by batch (plate) and color-coded by

biological replicate (mouse). The time point for each batch is indicated. Cells with less than 1,000 UMI were discarded from the analysis. **c,** Fraction of analyzed cells/batch after filtering. Batches are grouped and color-coded as described in **b**. **d,** Single cell RNA-seq data from 8987 QC positive cells staining negative for Ter119, CD45 and EpCAM was analyzed and clustered using the MetaCell algorithm, resulting in a two-dimensional projection of cells from 15 mice. 88 meta-cells were associated with 4 broad clusters, annotated and marked by color code. **e**, Expression of the hallmark genes for the 4 clusters presented in **d** on top of the two-dimensional projection of breast cancer stroma. Colors indicate log transformed UMI counts normalized to total counts per cell. **f,** Volcano plot displaying differentially expressed genes between *Pdpn*$^{+}$ fibroblasts and *S100a4*$^{+}$ fibroblasts (see also supplementary table 4). Marker genes for NMF, pCAF, and sCAF are highlighted. **g,** Fraction of cells originated from each mouse and subset, from all cells originated in their time point. Bar values represent the mean fraction values. Time points and subclasses are annotated and colored as in Fig. 1d. **h,** Squared Pearson correlation matrix between bulk and single cell sequencing results for NMF, pCAF, and sCAF.

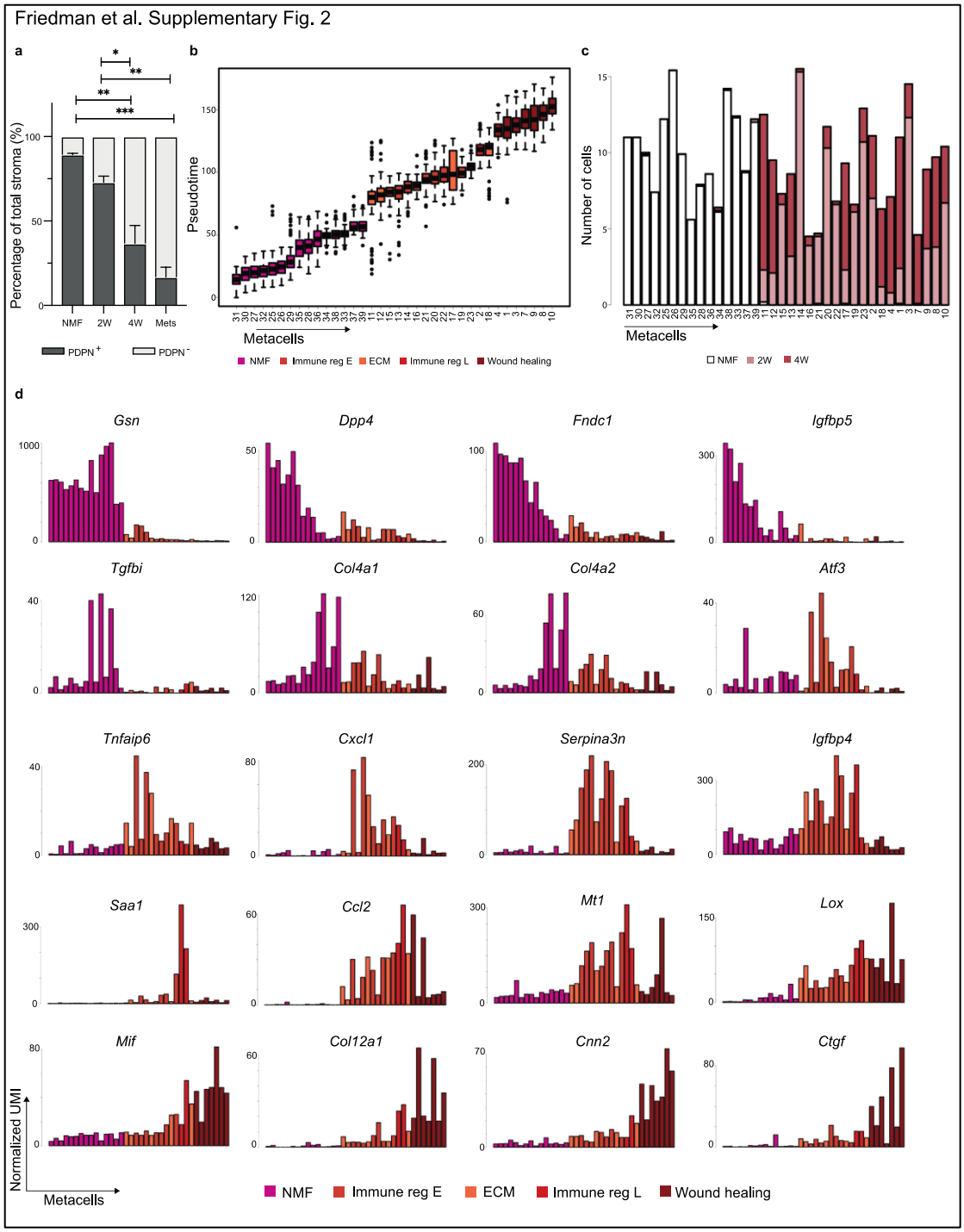

Supplementary Fig. 2: *Pdpn*⁺ fibroblasts undergo dynamic changes in gene expression and subset composition during tumor progression. a, Cell-surface PDPN protein expression levels obtained from index sorting data (presented in Fig. 1d, lower panel), were used to quantify the percent of PDPN^{+} and PDPN^{-} cells in the CD45^{-}EpCAM^{-} stroma in the different time points. P-value was determined by Anova considering multiple comparisons. **b,** Pseudo-time of expression for individual metacells (color coded by functional subclasses as in Fig. 2) included in the slingshot analysis. Box plots display median bar, first–third quartile box and 5th–95th percentile whiskers. **c,** Distribution of cells across time points (color coded) within metacells included in the slingshot analysis. Metacell numbers and order are consistent across all figure panels and match the order in Fig. 2. **d,** Expression of hallmark

NMF and pCAF genes (additional to those presented in Fig. 2e) across metacells (average UMI/cell), ordered by pseudo-time. * p<0.05; ** p<0.005; *** p<0.001

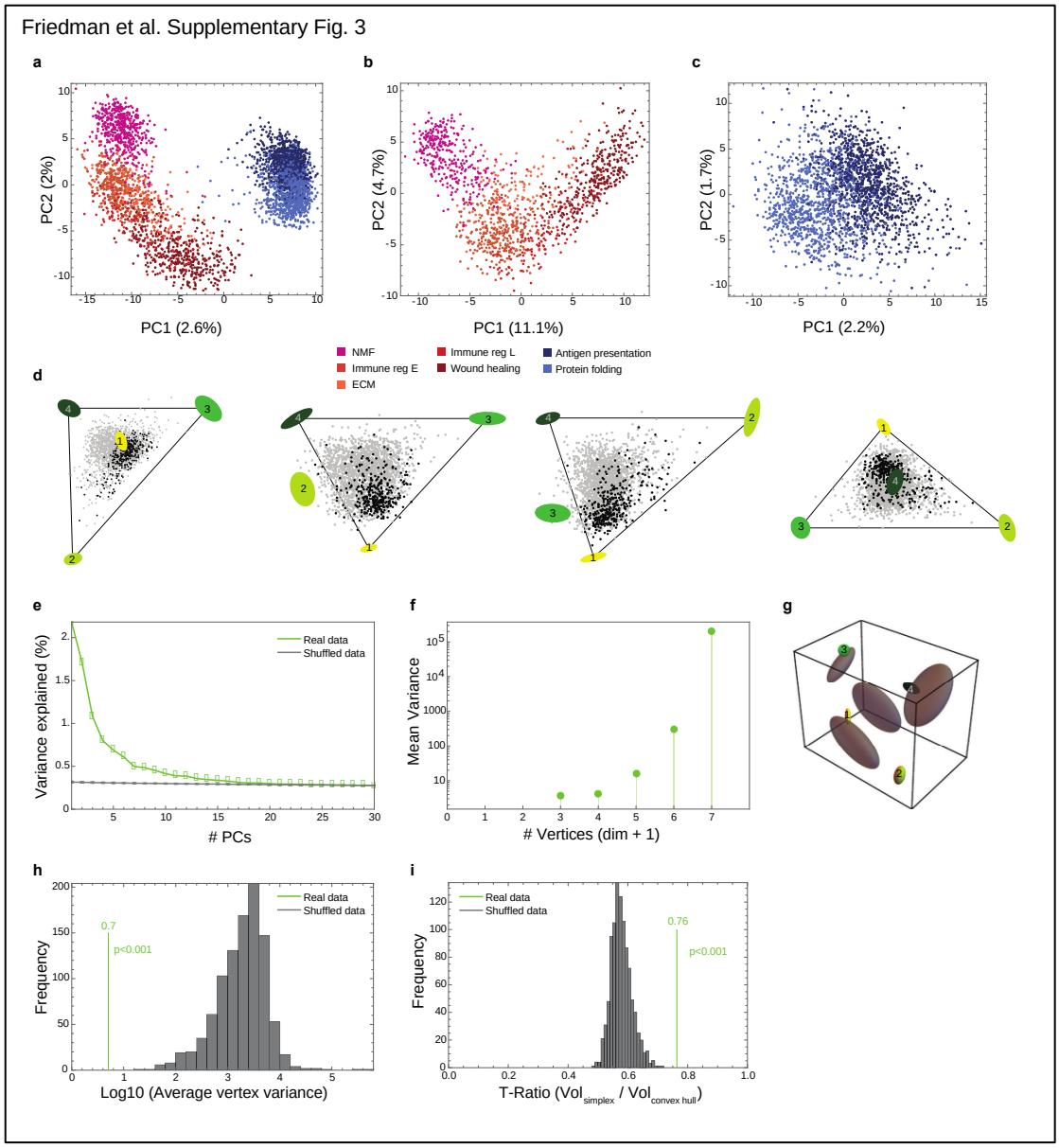

Supplementary Fig. 3: pCAFs and NMFs form a curve in gene-expression space, whereas a tetrahedron describes sCAF gene expression. a, PCA analysis of NMF, and pCAF and sCAF from 2W and 4W, color coded according to the subclasses defined in Fig. 1c. **b-c,** PCA analyses for NMF and pCAF (**b**) and for sCAF (**c**) color coded as in **a**. **d,** Data projected on the four faces of the tetrahedron. **e,** Explained variance as a function of the number of PCs (real data) vs. random. Note that the total variance explained by the first 3 PCs, about 5%, is typical of single-cell gene expression data[22]. **f,** Variance of vertex positions as a function of the number of vertices considered, using PCHA with k=3-7 vertices. **g,** Variation of vertex position (bootstrapping) for the real data (ellipses color-coded as in Fig. 3) *vs* shuffled data (grey ellipses). **h,** Histogram depicting the average variation of vertex positions calculated for the real data (green) *vs* multiple runs of shuffled data (grey). **i,** Histogram depicting the ratio between the volumes of the convex hull of the data and the minimal enclosing tetrahedron (t-ratio). The t-ratio of the real data (green) is compared to t-ratios of shuffled data (1000 shuffles; grey).

Friedman et al. Supplementary Fig. 4

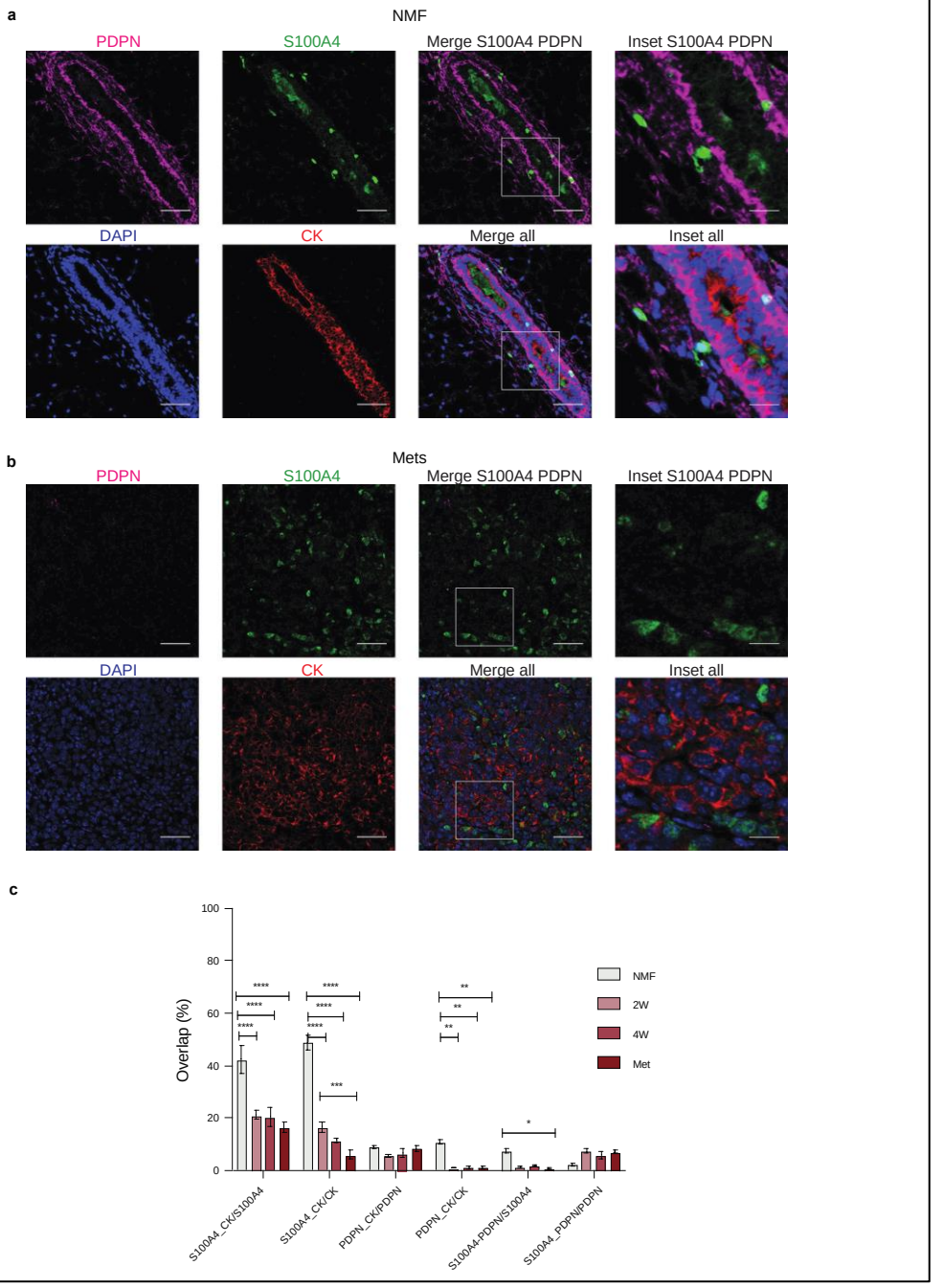

Supplementary Fig. 4: PDPN and S100A4 proteins mark distinct types of cells in mouse tumors, the majority of which are CK-negative. a-b, Representative images of normal mammary fat pads (NMF; **a**) and lung metastases (Mets; **b**) (see Fig. 4a) stained with antibodies against the indicated proteins. Scale bar = 50μm, inset scale bar = 17□m. **c,** Quantification of the average overlap between CK, PDPN, and S100A4 staining in NMFs, primary tumors (2W and 4W) and Mets. Bars represent the number of overlapping pixels between two channels, divided by the total number of pixels of the originating channels, averaged for 3 biological replicates (9 images per mouse). P-values were calculated by two-way Anova correcting for multiple comparisons. * p<0.05; ** p<0.005; *** p<0.001; *** p<0.0001

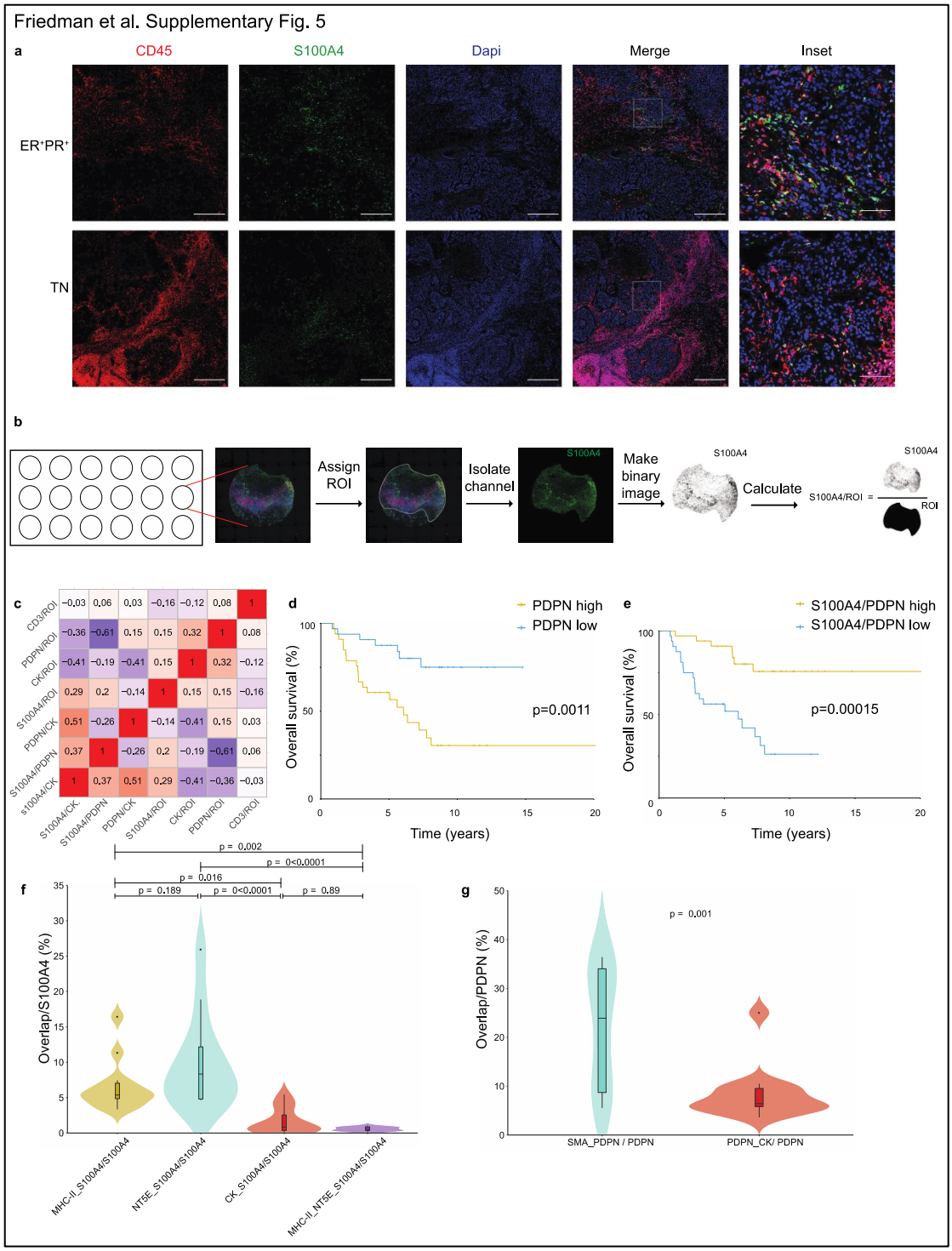

Supplementary Fig. 5: Low PDPN staining and high S100A4/PDPN staining ratios correlate with better overall survival of TNBC patients. a, Representative images of MxIF staining of serial sections from the same patients presented in Fig. 6a with antibodies against the indicated proteins. Scale bar = 500 □m.; inset scale bar = 90 □m **b,** Illustration of the image analysis workflow. **c,** Heat map showing Pearson's correlation coefficients of the staining scores for different cell type markers. **d-e,** The association with overall survival of PDPN (**d**) or S100A4/PDPN (**e**) scored and classified as in Fig. 6b was assessed by KM analysis. p Values were calculated using log rank test. **f-g,** The overlap between S100A4, CK, MHC-II and NT5E stains (**f**) and between PDPN, CK, and SMA stains (**g**) in a subset of

12 patients (average scores of 3 images per patient) of the TNBC is presented. P-values were calculated by two-way Anova (with correction for multiple comparisons in (**f**)).

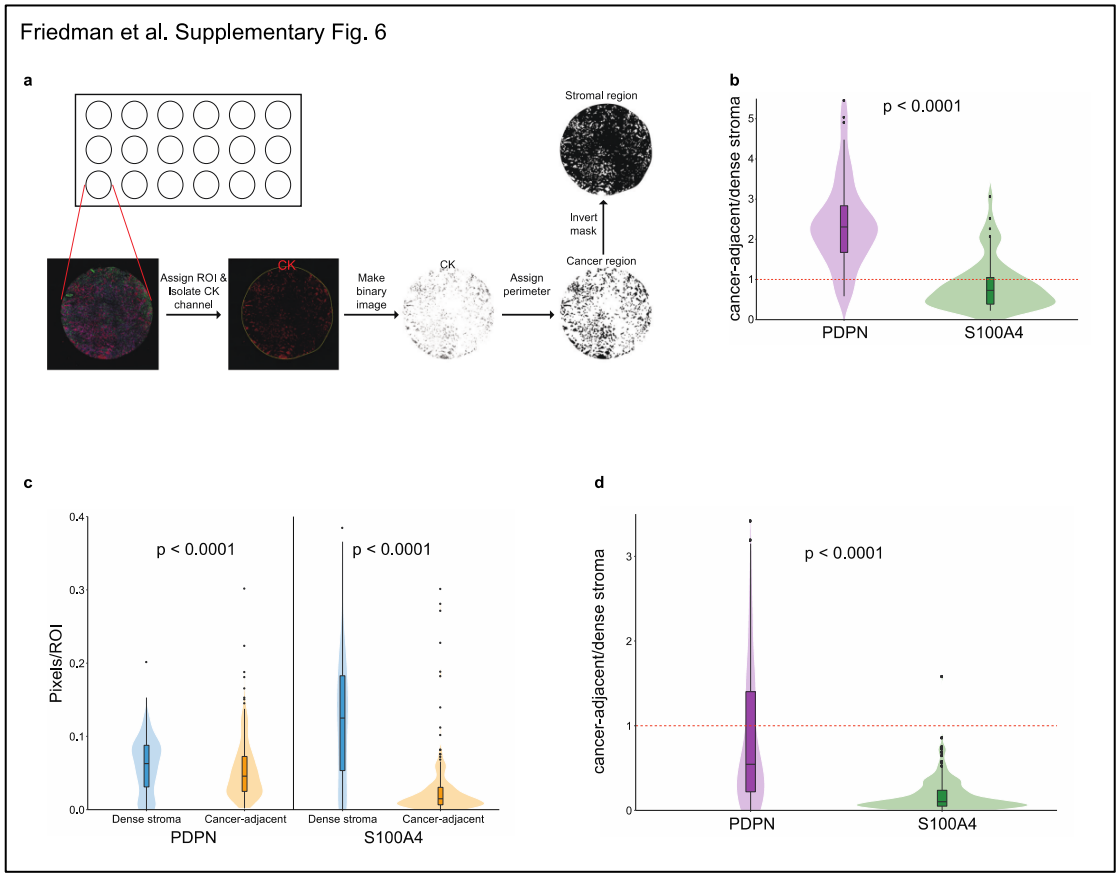

Supplementary Fig. 6: pCAFs tend to localize to cancer-adjacent regions more often than sCAFs in human breast cancer patients. a, Illustration of the regional analysis workflow. **b,** The ratio of cancer-adjacent/dense stroma PDPN and S100A4 staining was determined for each core in the TNBC TMA (See also Fig. 6d). P-value was calculated using Wilcoxon matched pairs signed rank test. **c-d,** Cancer-adjacent regions and regions of dense stroma were determined for each core in the METABRIC TMA based on CK staining (see Methods section), PDPN and S100A4 staining in each region was scored (**c**) and the ratio of cancer-adjacent/dense stroma PDPN and S100A4 staining was determined (**d**). P-values were calculated using Wilcoxon matched pairs signed rank test.

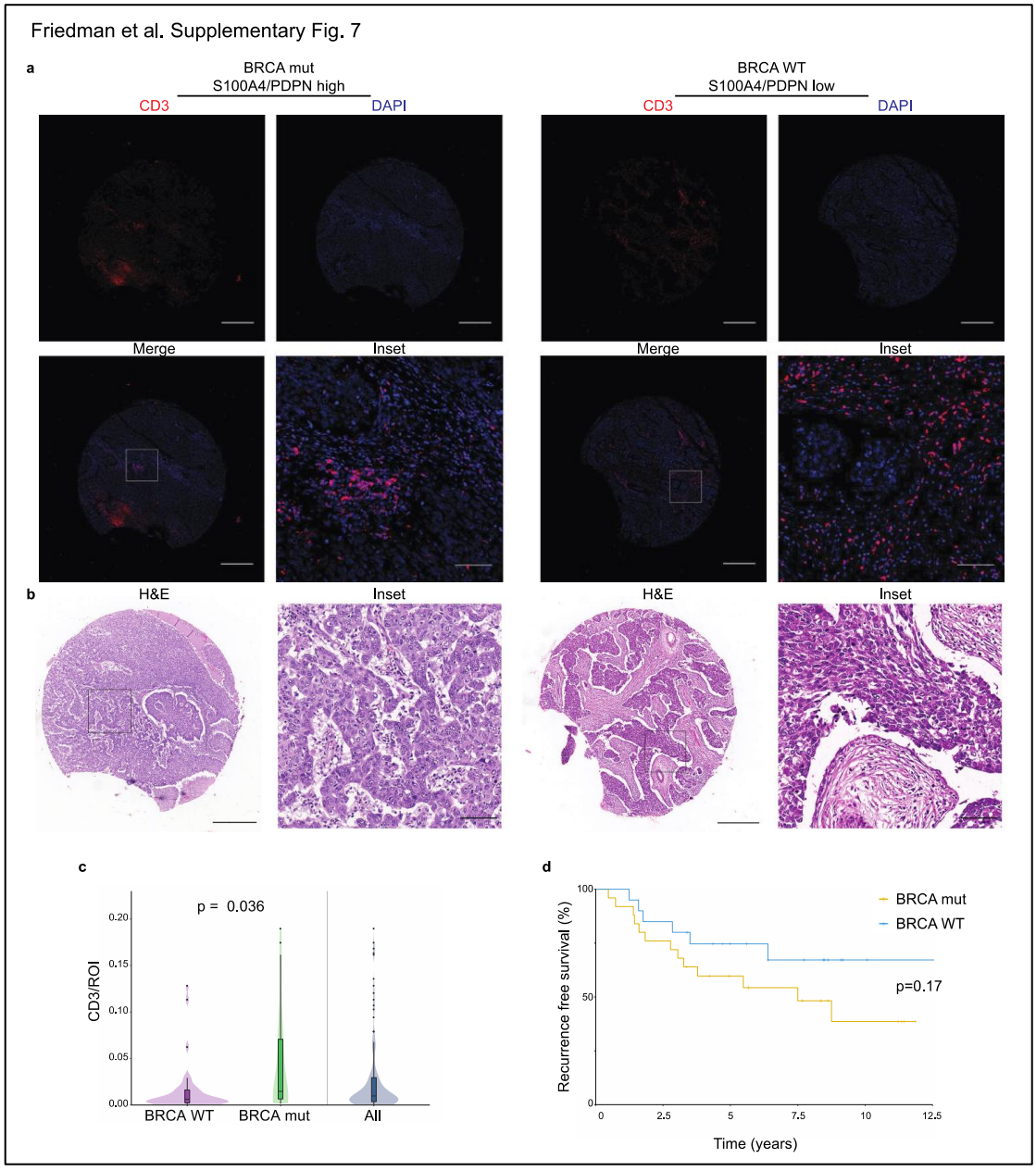

Supplementary Fig. 7: BRCA status is not significantly correlated with recurrence free survival in a cohort of TNBC patients. a-b, Representative images of CD3 and DAPI staining (**a**) and H&E stains (**b**) in a BRCA mutated (mut) patient and a BRCA WT patient from our cohort of 72 TNBC patients (Serial sections of the same cores used in Fig. 6a are shown). Scale bar = 500μm; inset scale bar = 80μm. **c,** Vase-box plot depicting CD3 staining scores (see Methods) in BRCA WT (n=25) *vs* BRCA mut (n=20) patients, as well as the total TNBC cohort (n=72). p Value was calculated using a student's t-test. **d,** 45 TNBC patients were stratified by BRCA mutational status and the association with recurrence free survival was assessed by KM analysis. P-value was calculated using log rank test.

Supplementary Table 1. Summary of biological samples

Mouse ID	Tissue	Batch num	n cells
m1	Normal mammary fat pad	1	207
m1	Normal mammary fat pad	2	143
m1	Normal mammary fat pad	3	209
m2	Normal mammary fat pad	4	204
m2	Normal mammary fat pad	5	174
m2	Normal mammary fat pad	6	114
m3	Normal mammary fat pad	7	188
m3	Normal mammary fat pad	8	92
m3	Normal mammary fat pad	9	195
m4	Primary tumor, 2 weeks post injection	10	243
m4	Primary tumor, 2 weeks post injection	11	233
m5	Primary tumor, 2 weeks post injection	12	255
m5	Primary tumor, 2 weeks post injection	13	244
m5	Primary tumor, 2 weeks post injection	14	243
m6	Primary tumor, 2 weeks post injection	15	213
m6	Primary tumor, 2 weeks post injection	16	167
m7	Primary tumor, 4 weeks post injection	17	96
m7	Primary tumor, 4 weeks post injection	18	60
m7	Primary tumor, 4 weeks post injection	19	65
m7	Primary tumor, 4 weeks post injection	20	38
m7	Primary tumor, 4 weeks post injection	21	60
m8	Primary tumor, 4 weeks post injection	22	218
m8	Primary tumor, 4 weeks post injection	23	193
m8	Primary tumor, 4 weeks post injection	24	231
m8	Primary tumor, 4 weeks post injection	25	229
m8	Primary tumor, 4 weeks post injection	26	236
m8	Primary tumor, 4 weeks post injection	27	237
m9	Primary tumor, 4 weeks post injection	28	144
m9	Primary tumor, 4 weeks post injection	29	144
m9	Primary tumor, 4 weeks post injection	30	116
m9	Primary tumor, 4 weeks post injection	31	129
m10	Primary tumor, 4 weeks post injection	32	165
m10	Primary tumor, 4 weeks post injection	33	136
m11	Primary tumor, 4 weeks post injection	34	81
m11	Primary tumor, 4 weeks post injection	35	156
m11	Primary tumor, 4 weeks post injection	36	39
m11	Primary tumor, 4 weeks post injection	37	136
m12	Primary tumor, 4 weeks post injection	38	92
m12	Primary tumor, 4 weeks post injection	39	121
m12	Primary tumor, 4 weeks post injection	40	219
m12	Primary tumor, 4 weeks post injection	41	258
m13	Lung metastases	42	128
m13	Lung metastases	43	112
m13	Lung metastases	44	118
m14	Lung metastases	45	217
m14	Lung metastases	46	198
m14	Lung metastases	47	212
m15	Lung metastases	48	200
m15	Lung metastases	49	92
m15	Lung metastases	50	33

Supplementary Table 5. Top 40 DE genes between EpCAM-GFP- sCAFs and EpCAM+GFP+ 4T1 cancer cells.

* Gene	**GFP-EpCAM-	**GFP-EpCAM+	**GFP+EpCAM-	**GFP+EpCAM+
Ccl3	12.4057137	7.53736747	0	0
Hdc	11.4576988	5.92221425	2.49605844	0
Ccl4	13.1592977	8.0952709	0.94731761	1.74952899
Serpina1b	10.4637127	2.77549865	1.51428295	0
Il13	9.99739237	3.66610358	0	0
Osm	9.88473918	3.37231169	0.94731761	0
Ramp2	11.1172711	5.21925309	3.36216697	1.36456784
Cyp11a1	9.74972947	4.11868813	0	0
Des	10.5811615	3.66610358	1.92023697	0.83793993
Ifitm1	10.4542694	3.66610358	2.2366874	0.83793993
Csf2rb	10.4174865	4.53723893	2.2366874	0.83793993
Cyp4b1	9.51858347	2.77549865	0.94731761	0
Gpx3	11.5223889	11.0727436	1.92023697	2.05310563
Serping1	11.5042001	4.67569914	3.36216697	2.05310563
Csf2rb2	10.7807219	4.67569914	1.51428295	1.36456784
Col3a1	11.0819377	4.67569914	2.49605844	1.74952899
Cdh13	9.2649728	5.02567036	2.2366874	0
Meg3	9.24685513	1.73935152	0	0
Cxcl12	9.21738513	4.46268418	0	0
Il4	9.16431816	3.79323816	0	0
Etv4	6.41711128	8.55157789	9.2808219	9.43222119
Krt14	7.75474804	10.9561468	7.87607232	10.7783469
Rhox5	6.39095167	8.97014622	7.20622205	9.44694654
C3	7.71312431	9.88553719	9.87716676	10.7757571
Msln	6.41711128	8.88349371	9.30642962	9.48232149
Mmp13	6.30950041	7.95952768	8.56179708	9.40231178
Tslp	6.22317397	9.24776549	8.36462742	9.34056589
Padi4	6.41711128	9.44461747	9.71453541	9.64157013
Il24	5.96399668	8.49658613	8.3275886	9.19308659
Lad1	6.7199833	9.3978649	9.15726209	9.95142293
Sfn	6.5172496	10.8218544	7.23317612	9.74977814
Cldn4	8.13171734	11.5909493	8.61400156	11.3842299
Kcnn4	6.5648274	9.5085525	8.96698651	9.82810914
Ankrd1	6.0993976	8.76051157	9.22596642	9.3905108
Mmp9	8.52956968	11.4795616	10.8115591	11.8584689
Spp1	10.23835	12.8797319	13.7380379	13.6181744
Tns4	6.33716494	8.93265869	9.96152033	9.79011695
Anxa8	6.03328503	9.38530556	8.7320854	9.49339766
Syt8	6.06671999	8.89771264	9.67248442	9.55057096
Gpa33	6.84086377	9.75884732	9.66425526	10.3350618

* 20 most upregulated and 20 most downregulated genes from all genes with a minimum of 2^8 average normalized reads (between GFP+EpCAM+ and GFP-EpCAM-; 1525 in total). Genes upregulated in EpCAM-GFP- are in orange; Genes upregulated in EpCAM+GFP+ are in blue.

** Reads are presented as log2 normalized values.

Supplementary Table 7. TNBC cohort clinical characteristics

Characteristic		
n		72
Age at Dx (mean)		55.97
Tumor size, n (%)*	T1	41 (60.3)
	T2	23 (33.8)
	T3	4 (5.9)
LN, n (%)	Negative	50 (72.5)
	Positive	19 (27.5)
Grade, n (%)	1	1 (1.4)
	2	9 (12.9)
	3	60 (85.7)
BRCA, n (%)	WT	25 (34.7)
	Mut	20 (27.8)
	Unknown	27 (37.5)

Supplementary Table 8. TNBC cohort univariate analyses

Variable (n)		Hazard Ratio	95% CI	P-Value
*CK (70)		36514.700		0.028
*Pdpn (70)		14019.614		0.013
S100A4 (70)		0.058	0 - 10075.709	0.644
CD3 (68)		4.539	0.058 - 356.571	0.497
S100A4/Pdpn (70)		0.388	0.199 - 0.758	0.005
Pdpn/CK (70)		0.956	0.861 - 1.065	0.424
S100A4/CK (70)		0.909	0.791 - 1.045	0.180
LN (69)		1.865	0.865 - 3.964	0.105
**Tumor size (69)	T1	1 [Reference]		
	T2	2.100	0.956 - 4.607	0.065
	T3	4.475	1.258 - 15.921	0.021
BRCA status (45)	WT	1 [Reference]		
	Mut	0.624	0.315 - 1.238	0.177
Age (72)		1.022	0.999 - 1.045	0.062

Supplementary Table 10. TNBC cohort Multiplicative Multivariate Analysis

Variable (n)	Hazard Ratio	95% CI	P-Value	Likelihood ratio test
S100A4/Pdpn (45)	0.828	0.421 - 1.631	0.585	
BRCA status (45)	37.101	4.000 - 344.491	0.001	
S100A4/Pdpn:BRCA (45)	0.015	0.001 - 0.230	0.002	< 0.001

Variable (n)	Hazard Ratio	95% CI	P-Value	Likelihood ratio test
Pdpn/Total ROI (45)	5.57E+05	0.6 - 5.058E+11	0.059	
BRCA status (45)	0.143	0.021 - 0.9692	0.046	
Pdpn/Total ROI:BRCA (45)	8.26E+12	2.778 - 2.45E+18	0.039	0.095

Supplementary Table 11. Antibodies and reagents

Antibody	Conjugation	Clone	Source	Cat#	Target species	Application
EpCAM	Alexa flour 488	G8.8	Biolegend	118210	mouse	FACS analysis and sorting
EpCAM	FITC	G8.8	eBioscience	11579182	mouse	FACS analysis and sorting
CD45	BV711	30-F11	Biolegend	103147	mouse	FACS analysis and sorting
CD45	APC	30-F11	Biolegend	103112	mouse	FACS analysis and sorting
Ter119	Pacific blue	Ter119	Biolegend	116232	mouse	FACS analysis and sorting
PDPN	APC	8.1.1	Biolegend	127410	mouse	FACS analysis and sorting
PDPN	APC/Cy7	8.1.1	Biolegend	127417	mouse	FACS analysis and sorting
PDPN	biotin	8.1.1	Biolegend	127404	mouse	FACS analysis and sorting
Propidium iodide	-	-	Sigma Aldrich	P4170	mouse	FACS analysis and sorting
S100A4	-	polyclonal	Abcam	ab41532	mouse, human	Immunofluoresence
PDPN	-	polyclonal	R&D Systems	AF3244	mouse	Immunofluoresence
PDPN	-	D2-40	Biolegend	916605	human	Immunofluoresence
Cytokeratin 7	-	EPR17078	Abcam	ab181598	mouse	Immunofluoresence
Pan-cytokeratin	-	AE1/AE3	Dako	M3515	human	Immunofluoresence
DAPI	-	-	Biolegend	422801	-	Immunofluoresence
CD3	-	D4V8L	Cell Signaling	99940	human	Immunofluoresence
CD45	-	D9M8I	Cell Signaling	13917	human	Immunofluoresence
Ly-6C	PerCP/Cy5.5	HK 1.4	Biolegend	128011	mouse	FACS analysis and sorting
I-A/I-E	APC/Cy7	M5/114.15.2	Biolegend	107628	mouse	FACS analysis and sorting
HLA-DR	-	EPR3692	Abcam	ab92511	human	Immunofluoresence
α-SMA	-	1A4	Sigma Aldrich	A2547	huma/mouse	Immunofluoresence
α-SMA	FITC	1A4	Sigma Aldrich	F3777	huma/mouse	FACS analysis
NT5E/CD73	-	D7F9A	Cell Signaling	13160	human	Immunofluoresence
Bovine anti-Goat	HRP	polyclonal	Jackson	805-035-180	goat	Immunofluoresence
Goat anti-Rabbit	HRP	polyclonal	Jackson	111-035-144	rabbit	Immunofluoresence
Goat anti-Mouse	HRP	polyclonal	Abcam	97040	mouse	Immunofluoresence
Opal 520 Reagent	Opal 520	-	PE	FP1487001KT	-	Immunofluoresence
Opal 570 Reagent	Opal 570	-	PE	FP1488A	-	Immunofluoresence
Opal 620 Reagent	Opal 620	-	PE	FP1495	-	Immunofluoresence
Opal 650 Reagent	Opal 650	-	PE	FP1496A		Immunofluoresence
Opal 690 Reagent	Opal 690		PE	FP1497A	-	Immunofluoresence
1X Plus Amp Diluent	-	-	PE	FP1498	-	Immunofluoresence

Supplementary Table 12. Selected genes, priority, and fold change threshold for subset specific gene expression analysis

Group	Gene	Priority	T_fold
Wound healing	Acta2	6	4.1
Immune regulatory E	Cxcl12	9	4.9
ECM	Mfap5	5	8.2
NMF	Gsn	5	18
Inflammatory A	Cxcl1	4	3.5
Immune regulatory L	Saa3	7	15
Inflammatory B	Il6	17	5
Antigen presentation	Spp1	7	3.1
Protein folding	S100a4	13	1.77